

Observables for the Analysis of Event Shapes in e^+e^- Annihilation and Other Processes

Geoffrey C. Fox and Stephen Wolfram

California Institute of Technology, Pasadena, California 91125

(Received 18 September 1978)

We present a set of rotationally invariant observables which characterizes the "shapes" of events, and is calculable in quantum-chromodynamics perturbation theory for final states consisting of quarks and gluons (G). We include the effects of fragmentation to hadrons in comparing the shapes of events from the processes $e^+e^- \rightarrow q\bar{q}$, $e^+e^- \rightarrow q\bar{q}G$, and $e^+e^- \rightarrow \text{heavy resonance} \rightarrow GGG$, and from heavy-quark and lepton production. We indicate how our analysis may be extended to deep-elastic lepton-hadron interactions and hadron-hadron collisions involving large transverse momenta.

Experiments¹ have shown that at high center-of-mass energies (\sqrt{s}) the final states in $e^+e^- \rightarrow \text{hadrons}$ usually consist predominantly of two jets of hadrons presumably resulting from the process $e^+e^- \rightarrow q\bar{q}$. Quantum chromodynamics (QCD) explains this basic two-jet structure,² but predicts that one of the outgoing quarks should sometimes emit a gluon (G), tending to lead to three-jet final states.

Previous attempts³ to discriminate between two- and three-jet events concentrated on finding a "jet axis" by minimization, and then measuring the collimation of particles with respect to it.

Instead, one may use observables which directly characterize the "shape" of each event. Since there is no natural axis defined in the final state of e^+e^- annihilation, it is convenient to consider rotationally invariant observables. A set of such observables is given by [$Y_l^m(\Omega)$ are the usual spherical harmonics and $P_l(\cos\varphi)$ the Legendre polynomials]

$$H_l \equiv \left(\frac{4\pi}{2l+1} \right) \sum_{m=-l}^{+l} \left| \sum_i Y_l^m(\Omega_i) \frac{|\vec{p}_i|}{\sqrt{s}} \right|^2$$

$$= \sum_{i,j} \frac{|\vec{p}_i| |\vec{p}_j|}{s} P_l(\cos\varphi_{ij}), \quad (1)$$

where the indices i and j run over the hadrons which are produced in the event, and φ_{ij} is the angle between particles i and j . When the first for the H_l is used, one must choose a particular set of axes to evaluate the angles (Ω_i) of their momenta, but the values of the H_l deduced will be independent of the choice. Energy-momentum conservation requires $H_1=0$ and $H_0=1$. In principle, all the other H_l carry independent information.⁴ In practice, however, one need only consider the lower-order H_l ; in this paper we concentrate on H_2 and H_3 .

The information contained in the H_l may also be expressed by the "autocorrelation function"

$$F(\cos\beta) = 2 \int \rho(\hat{\Omega}) \rho(\hat{\Omega}\hat{R}(\alpha, \beta, \gamma)) \\ = \sum_l (2l+1) H_l P_l(\cos\beta), \quad (2)$$

where $\rho(\hat{\Omega})$ is a continuous distribution of momentum and $\hat{\Omega}, \hat{R}$ are operators in the rotation group. For particle events, we define the two-detector energy correlation⁵

$$\tilde{F}_2(\sigma_1, \sigma_2) = \frac{16\pi^2}{|\sigma_1||\sigma_2|} \frac{E_1 E_2}{s}, \quad (3)$$

where E_i are energies incident on detectors covering the regions σ_i of total solid angle $|\sigma_i|$. We form the rotationally invariant observable F_2 by averaging \tilde{F}_2 over all possible positions for the detectors, while maintaining their relative orientation. In e^+e^- annihilation events, this may be achieved (apart from correlations with the beam axis and polarization) by averaging over events. In the limit $|\sigma_i| \rightarrow 0$, F_2 becomes a function solely of the angle β between the two point detectors, and is identical to $F(\cos\beta)$. F_2 may clearly be generalized to a correlation between n detectors (F_n). However, unlike the case of the H_l , there are infrared difficulties when the F_n are calculated in QCD perturbation theory.⁶

The ability of the H_l to distinguish between different processes is illustrated in Fig. 1. Final states of the process $e^+e^- \rightarrow q\bar{q}$ have $H_l=1$ for even l and $H_l=0$ for odd l . In contrast, the process $e^+e^- \rightarrow q\bar{q}G$ gives events with a wide distribution of H_l values, corresponding to a range of shapes. For example, the dependence of H_2 on the fractional energies $x_i (=2E_i/\sqrt{s})$ of the final quarks and gluons in this case is given by

$$H_2 = 1 - 6(1-x_1)(1-x_2)(1-x_3)/x_1x_2x_3. \quad (4)$$

Each kinematic configuration, labeled by the x_i , leads to an event of a different shape, and each is characterized by a particular value of H_2 .

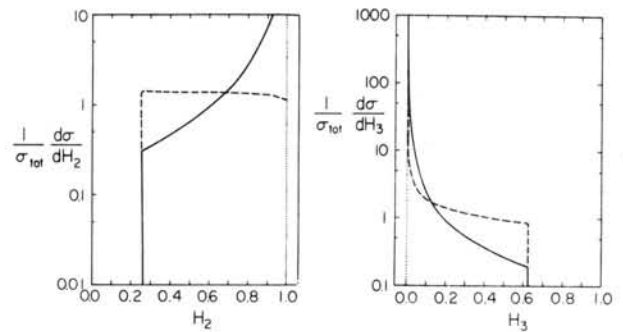


FIG. 1. The distributions in H_2 and H_3 for the processes $e^+e^- \rightarrow q\bar{q}$ (dotted lines), $e^+e^- \rightarrow q\bar{q}G$ (full lines), and $e^+e^- \rightarrow \text{heavy resonance} \rightarrow GGG$ (dashed lines). The process $e^+e^- \rightarrow q\bar{q}G$ alone yields an infinite total cross section, but when added to $e^+e^- \rightarrow q\bar{q}$ calculated through $O(g^2)$ the combination of processes [denoted by $e^+e^- \rightarrow q\bar{q}(G)$] gives a finite cross section. We have taken $\alpha_s = 0.25$ for the $e^+e^- \rightarrow q\bar{q}G$ distribution.

The H_l do not discriminate between final states differing by the inclusion of a very low-energy particle or by the replacement of one particle by two collinear particles with the same total momentum. It is believed that these properties are sufficient to ensure that calculations involving the H_l are infrared finite in QCD perturbation theory.^{3,6}

A convenient measure of the event shapes due to different processes is provided by the mean H_l . For the sum of the process $e^+e^- \rightarrow q\bar{q}G$ and $e^+e^- \rightarrow q\bar{q}$ calculated to lowest order in the QCD coupling constant $\alpha_s = g^2/4\pi$, we have

$$\langle H_2 \rangle = 1 + (2\alpha_s/3\pi)(33 - 4\pi^2) \simeq 1 - 1.4\alpha_s, \quad (5)$$

so that a center-of-mass energy $\sqrt{s} = 40$ GeV, $\langle H_2 \rangle \simeq 0.76$.

QCD suggests that heavy $Q\bar{Q}$ vector mesons (such as ψ, Υ) should decay to three gluons. Figure 1 shows that the H_2 and H_3 distributions due to this process are very different from those for $e^+e^- \rightarrow q\bar{q}G$. The flatter H_2 distribution for the GGG decay is reflected in a lower $\langle H_2 \rangle$:

$$\langle H_2 \rangle \simeq \frac{103\pi^2 - 1008}{16(\pi^2 - 9)} \simeq 0.62. \quad (6)$$

Our results above were obtained by making the idealization that final states consist of free quarks and gluons. In reality, one must consider the "fragmentation" of these quarks and gluons into hadrons, although at sufficiently high energy the values of the H_l should be the same whether they are calculated from Eq. (1) using the momenta of the actual hadrons in each event, or of their par-

ent quarks and gluons. In order to estimate the shapes of realistic events at finite energy, one must go beyond the realms of present QCD theory and adopt an essentially phenomenological model for the generation of complete hadronic final states by the fragmentation of quarks and gluons. We use the model developed by Field and Feynman,⁷ which agrees with available data.⁸

QCD predicts that, away from resonances, e^+e^- annihilation should be dominated by the processes $e^+e^- \rightarrow q\bar{q}$ and $e^+e^- \rightarrow q\bar{q}G$. The processes $e^+e^- \rightarrow q\bar{q}G$ can give rise to final states containing either two or three jets of hadrons. Two-jet events occur when some of the quarks and gluons have low energy or are nearly collinear⁹ and they cannot be distinguished from $e^+e^- \rightarrow q\bar{q}$ events by measurements on the hadron final state. Only when $e^+e^- \rightarrow q\bar{q}G$ and $e^+e^- \rightarrow q\bar{q}$ [calculated through $O(g^2)$] are added is the jet-production cross section infrared finite. We denote this combination of processes by $e^+e^- \rightarrow q\bar{q}(G)$.

In Fig. 2, we present the H_2 distributions for realistic hadronic events resulting from $e^+e^- \rightarrow q\bar{q}$, $e^+e^- \rightarrow q\bar{q}(G)$, and $e^+e^- \rightarrow \xi - GGG$ (ξ is a heavy $Q\bar{Q}$ resonance). The modifications to the results in Fig. 1 due to the fragmentation of the quarks and

gluons into hadrons are striking. (They also occur for the higher H_i and for other observables designed to identify three-jet events.³) Nevertheless, above $\sqrt{s} \approx 10$ GeV, the H_2 distributions for the different types of events are clearly distinguished. By $\sqrt{s} \approx 40$ GeV, the predictions are similar to those obtained in the idealization of free quarks and gluons (Fig. 1). H_2 and H_4 distributions are particularly effective at distinguishing $e^+e^- \rightarrow q\bar{q}(G)$ and $e^+e^- \rightarrow \xi - GGG$ events, while H_3 distributions are very sensitive to the presence of any pure $e^+e^- \rightarrow q\bar{q}$ component. The H_1 distributions for realistic events may be made more similar to the idealized ones of Fig. 1 by using only the higher-momentum hadrons in each event for the computation of the H_i .¹⁰ Even the cut $|p_i| > 0.5$ GeV is sufficient to effect a great improvement. The H_i distributions¹⁰ are little affected if only the charged particles in each event are detected. Our predictions are not particularly sensitive to the parameters of the jet development model (which may presumably in any case be determined from single-hadron momentum distributions), but it is still difficult to estimate the uncertainties in our results at energies where the fragmentation of the quarks and gluons has an important effect. Refinement of the jet model as further experimental data become available should allow more accurate predictions to be made.

The H_i are not specialized to the investigation of two- and three-jet events. They may also be used to identify events of other types. The pair production and weak decay of heavy mesons (containing a heavy quark Q and a light antiquark \bar{q}) and heavy leptons (L) should give events containing many hadron jets. For heavy leptons we assume the decay scheme $L \rightarrow \nu_L u\bar{d}$, while for heavy quarks (mesons) we consider the three possibilities $Q \rightarrow q' u\bar{d}$, $Q \rightarrow q' G$, and $Q\bar{q}_{\text{spect}} \rightarrow q'\bar{q}''$. Figure 3 shows our predictions for the H_2 distributions of heavy-quark and lepton production events. We take no account of hadron production by heavy quarks prior to their weak decays, so that our results for heavy-quark pair production should be valid only near threshold.

In addition to the H_i , one may consider the multipole moments⁵

$$B_i \equiv \sum_i (|\bar{p}_i|/\sqrt{s}) P_i(\cos \alpha_i), \quad (7)$$

where α_i are the angles made by the particles in the event with the beam axis. A $q\bar{q}$ final state with angular distribution $1 + \lambda \cos^2 \alpha_i$ (the naive parton model predicts $\lambda = 1$) gives a broad dis-

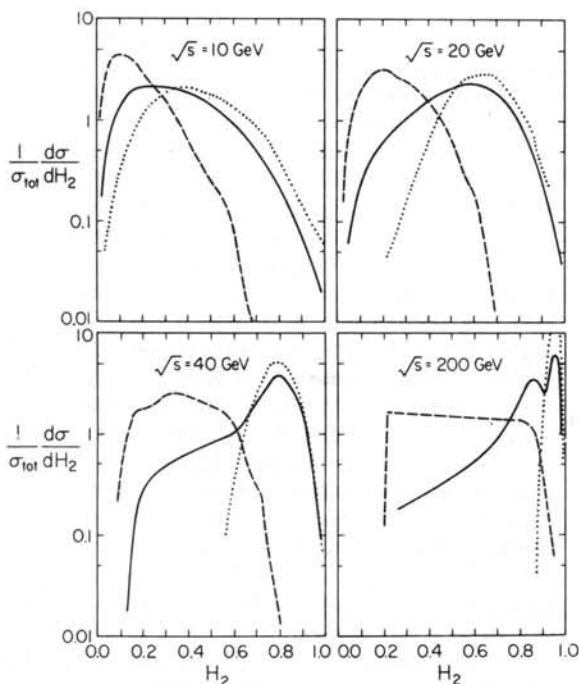


FIG. 2. The H_2 distributions predicted for hadronic events resulting from the processes $e^+e^- \rightarrow q\bar{q}$ (dotted lines), $e^+e^- \rightarrow q\bar{q}(G)$ (full lines), and $e^+e^- \rightarrow \text{heavy resonance} \rightarrow GGG$ (dashed lines), at various center-of-mass energies \sqrt{s} .

tribution in B_2 with mean $2\lambda/5(\lambda+3)$, while the process $e^+e^- \rightarrow q\bar{q}(G)$ gives $\langle B_2 \rangle \approx 1/10 - 3\alpha_s/10\pi$, corresponding to $\lambda \approx 1 - 4\alpha_s/\pi$, and $e^+e^- \rightarrow \zeta - GGG$ gives $\langle B_2 \rangle \approx (72 - 7\pi^2)/80(\pi^2 - 9)$ or $\lambda \approx (72 - 7\pi^2)/(13\pi^2 - 120) \approx 0.35$. The H_i , being rotational invariants, are of course insensitive to correlations with the beam direction. They are, however, far superior in identifying the shape of events and distinguishing competing processes.

The H_i may also be used to analyze three-jet effects in deep-inelastic lepton-nucleon scattering. Making the idealization of free final quarks and gluons, and treating the nucleon fragments as a single particle, we find that in the virtual photon- (or W -) nucleon rest frame, two-jet events arising from $\gamma^*q \rightarrow q$ give $H_1 \approx 1$ for even l and $H_1 \approx 0$ for odd l , just as in e^+e^- annihilation. The three processes¹¹ $\gamma^*q \rightarrow q$, $\gamma^*q \rightarrow qG$, and $\gamma^*G \rightarrow q\bar{q}$ typically give a $\langle H_2 \rangle$ which varies smoothly from $1 - 0.5\alpha_s$ at Bjorken x around 0.1 to $1 - 0.9\alpha_s$ at $x = 0.8$. The distributions in the H_i are similar to those in e^+e^- annihilation. The effects of fragmentation to hadrons are governed by $s_{\gamma^*N} = Q^2(1/x - 1)$.

For processes in which a natural plane (Π) is defined it is convenient to use the two-dimensional analogs of the H_i :

$$C_i \equiv \left| \sum_i \frac{|\vec{p}_i|_{\text{proj}}}{\sqrt{s}} \exp(i\varphi_i) \right|^2, \quad (8)$$

where φ_i are the angles of the particles relative to an arbitrary axis in Π , and $|\vec{p}_i|_{\text{proj}}$ are the

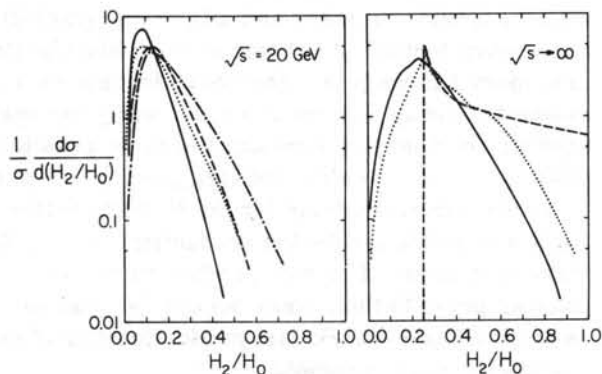


FIG. 3. The H_2 distributions predicted for hadronic events resulting from the production and weak decay of heavy-quark (Q) and -lepton (L) pairs (dotted lines) at $\sqrt{s} = 20$ GeV, and in the free-quark and gluon approximation ($\sqrt{s} \rightarrow \infty$). Three mechanisms for heavy-quark decay are considered: $Q \rightarrow q' u\bar{d}$ (full lines, $Q \rightarrow q' G$ (dashed lines), and $Q\bar{q}_{\text{spect}} \rightarrow q' \bar{q}''$ (dot-dashed lines). In the free-quark and gluon approximation the latter two processes give the same H_i distributions.

magnitudes of their momenta projected onto Π . In deep-inelastic scattering, it is best to take the plane Π to be orthogonal to the γ^* (or W^*) direction. Then two-jet events give $C_1 \approx 0$, while three-jet ones can give nonzero values of C_{21} .¹² Typically, in the free-quark approximation, $\langle C_{21} \rangle$ is independent of l , and typically $\langle C_{21} \rangle \approx 0.06\alpha_s$ at $x = 0.1$, rising to $0.15\alpha_s$ at $x = 0.8$. In hadron-hadron collisions involving high transverse momenta, Π should be chosen as the plane perpendicular to the incoming hadrons. Once again, the distributions in C_i/C_0 distinguish two- and three-jet events. The obvious two-dimensional analog of F_2 [as defined in Eq. (2)] will also be useful.

A detailed discussion of the work summarized here is given in Ref. 6.

This work was supported in part by the U. S. Department of Energy under Contract No. EY 76-C-03-0068. We are grateful to R. D. Field and R. P. Feynman for the use of their jet-development computer program, and to the MATHLAB group of the Massachusetts Institute of Technology Laboratory for Computer Science for the use of MACSYMA.

¹See, for example, B. H. Wilk and G. Wolf, DESY Report No. 78-23, 1978 (to be published).

²G. Sterman and S. Weinberg, Phys. Rev. Lett. **39**, 1436 (1977); G. Sterman, Phys. Rev. D **17**, 2789 (1978).

³H. Georgi and M. Machacek, Phys. Rev. Lett. **39**, 1237 (1977); E. Farhi, Phys. Rev. Lett. **39**, 1587 (1977); A. De Rújula, J. Ellis, E. G. Floratos, and M. K. Gaillard, Nucl. Phys. **B138**, 387 (1978); S.-Y. Pi, R. L. Jaffe, and F. E. Low, Phys. Rev. Lett. **41**, 142 (1978). These observables appear to be inconvenient to measure experimentally [S. Brandt and H. D. Dahmen, Seigen Report No. SI-78-8, 1978 (to be published)].

⁴The H_i may be generalized by taking n multipole moments of $\rho(\hat{\Omega})$ and combining them to give scalars under the rotation group using $3-j$ symbols. The set of all such observables determines $\rho(\hat{\Omega})$ up to an overall rotation. As we shall describe elsewhere, these observables allow precise tests for planes of particles in events. An obvious application is to $e^+e^- \rightarrow \zeta \rightarrow GGG$.

⁵The mean values of the B_i and \tilde{F}_2 for $e^+e^- \rightarrow q\bar{q}(G)$ have also been considered from a rather different point of view in C. L. Basham, L. S. Brown, S. D. Ellis, and S. T. Love, Phys. Rev. D **17**, 2298 (1978), and Phys. Rev. Lett. **41**, 1585 (1978) (this issue).

⁶G. C. Fox and S. Wolfram, California Institute of Technology Report No. CALT-68-678, 1978 (to be published).

⁷R. D. Field and R. P. Feynman, Nucl. Phys. **B136**, 1 (1978).

⁸The model was adjusted so as to agree with observed single-hadron momentum distributions. Limited experimental tests of its predictions for the detailed structure of jets [W. G. Scott, in "Neutrinos—78," edited by Earle C. Fowler (Perdue Univ. Press, to be published)] have proved successful.

⁹The division between configurations of quarks and gluons which give two- and three-jet events is determined by the details of their fragmentation to hadrons. At present the division must be made almost arbitrarily, but our results are not sensitive to the choice (see Ref. 6).

¹⁰If incomplete final states are considered then only a

fraction of the true energy of the event will be measured, so that it is convenient to use the effective H_1/H_0 rather than H_1 for this case.

¹¹All processes of $O(g^2)$, including those involving extra initial-state particles (e.g., $\gamma^*Gq \rightarrow q$), must be added in order to obtain an infrared-finite result. To $O(g^2)$, however, only the three-jet parts of $\gamma^*q \rightarrow qG$ and $\gamma^*G \rightarrow q\bar{q}$ contribute to $\langle H_{2l+1} \rangle$ and $\langle H_{2l} \rangle - 1$. $\gamma^*G \rightarrow q\bar{q}$ gives an insignificant contribution.

¹²One may also define two-dimensional analogs of the B_l . These provide an improved formulation of the tests of QCD proposed by H. Georgi and H. D. Politzer, Phys. Rev. Lett. 40, 3 (1978).